

## Air lasing by population inversion in $N_2^+$ induced by strong-field coherent coupling of the X, A and B states

(<sup>1</sup>*School of Science, The University of Tokyo*, <sup>2</sup>*Jilin University*) ○Erik Lötstedt,<sup>1</sup> Youyuan Zhang,<sup>1</sup> Toshiaki Ando,<sup>1</sup> Atsushi Iwasaki,<sup>1</sup> Huailiang Xu,<sup>2</sup> Kaoru Yamanouchi<sup>1</sup>

**Keywords:** air lasing, strong-field excitation, molecular dynamics, numerical simulation

When an intense, femtosecond near-IR laser pulse is focused in air, a short ( $\sim 1$  cm) plasma column called a filament is formed by the interplay between self-focusing and strong-field plasma defocusing. From the filament, unidirectional, coherent, and narrow-bandwidth radiation in the visible and UV wavelength range is emitted, which is referred to as air lasing. The emission at 391 nm, corresponding to the  $B^2\Sigma_u^+(v'=0) \rightarrow X^2\Sigma_g^+(v''=0)$  transition in  $N_2^+$  (see Fig. 1), has been intensively studied in the past decades, because the air lasing at 391 nm can be produced in a wide range of experimental conditions.

However, until 2015, the mechanism and the time scale of the formation of the population inversion between  $B^2\Sigma_u^+(v'=0)$  and  $X^2\Sigma_g^+(v''=0)$  of  $N_2^+$ , resulting in the air lasing at 391 nm, had not been understood well. In 2015<sup>1</sup>, we revealed both experimentally and theoretically that the abrupt exposure of  $N_2^+$  to the strong laser field, which is referred to as a sudden turn-on mechanism, combined with the population pumping from  $X^2\Sigma_g^+(v''=0)$  to  $A^2\Pi_u(v'=0)$  of  $N_2^+$ , is responsible for the population inversion and that the population inversion is built up on a femtosecond time scale. In the theoretical model, we consider the time-dependent Schrödinger equation (TDSE) for the nuclear wave packets in the  $X^2\Sigma_g^+$ ,  $A^2\Pi_u$ , and  $B^2\Sigma_u^+$  states,

$$i\hbar \frac{\partial}{\partial t} \begin{pmatrix} \psi_X(r,t) \\ \psi_A(r,t) \\ \psi_B(r,t) \end{pmatrix} = [T + V - \mathbf{E}(t) \cdot \boldsymbol{\mu}] \begin{pmatrix} \psi_X(r,t) \\ \psi_A(r,t) \\ \psi_B(r,t) \end{pmatrix}, \quad (1)$$

where  $r$  is the internuclear distance,  $\psi_k(r,t)$  is the nuclear wave packet in the electronic state  $k$ ,  $T$  is the kinetic energy operator,  $V$  is a  $3 \times 3$  matrix having the potential energy curves of the  $X^2\Sigma_g^+$ ,  $A^2\Pi_u$ , and  $B^2\Sigma_u^+$  states on the diagonal,  $\mathbf{E}(t)$  is the laser field, and  $\boldsymbol{\mu}$  is a  $3 \times 3$  matrix containing the dipole transition matrix elements. By numerically solving the TDSE, we showed that the population inversion can be explained by the following two mechanisms: (i) after ionization,  $N_2^+$  starts interacting immediately with the intense laser pulse, which efficiently induces the population transfer from the  $X^2\Sigma_g^+$  state to the  $B^2\Sigma_u^+$  state, and (ii) because of the near-resonant  $A^2\Pi_u$ - $X^2\Sigma_g^+$  coupling, a population is efficiently transferred to the  $A^2\Pi_u$  state, which promotes further the population inversion between the  $B^2\Sigma_u^+$  state and the  $X^2\Sigma_g^+$  state.

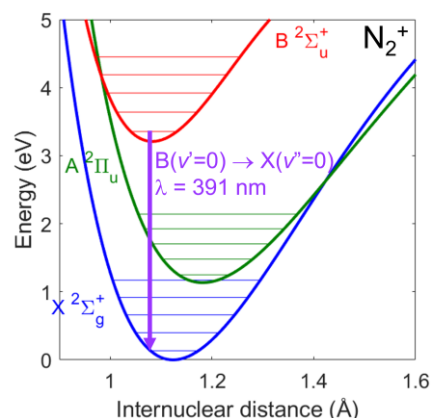


Fig. 1. Potential energy curves of  $N_2^+$ .

In 2019, we conducted pump-probe experiments<sup>2</sup> and showed that the  $B^2\Sigma_u^+(v' = 0) \rightarrow X^2\Sigma_g^+(v'' = 0)$  lasing signal at 391 nm oscillates as a function of the pump-probe delay time at the frequencies corresponding to the energy differences between the vibrational states in the  $X^2\Sigma_g^+$  state and those in the  $A^2\Pi_u$  state, which can be regarded as direct evidence that the mechanism of the excitation and lasing process of  $N_2^+$  is the coherent V-shaped  $A^2\Pi_u - X^2\Sigma_g^+ - B^2\Sigma_u^+$  coupling. Recently, we further showed<sup>3</sup> that the rotational coherence created in  $N_2^+$  can be clearly seen in the pump-probe delay-time dependence of the lasing signal at 391 nm. Indeed, the rotational structure of the lasing emission at 391 nm exhibited two maxima in the R-branch emission and the two maxima moved towards the longer wavelength as the delay time increases. By extending our theoretical model by including the rotational degree of freedom of  $N_2^+$ , we showed theoretically that the delay-time dependence of the R-branch emission spectrum can be interpreted as a temporal evolution of a rotational wave packet created in the  $B^2\Sigma_u^+$  state.

In order to use the air lasing for practical applications such as stand-off spectroscopic measurements and remote sensing, it is prerequisite to increase further the lasing emission intensity. We demonstrated experimentally<sup>4</sup> that the air lasing signal at 391 nm can be enhanced by two orders of magnitude by employing a polarization-gated IR laser pulse having a time-dependent polarization direction. At the peak of the pulse, an aligned  $N_2^+$  ensemble is created by the strong-field ionization, and during the latter half of the laser pulse, the polarization direction is changed so that the population transfer from  $X^2\Sigma_g^+$  to  $A^2\Pi_u$  is promoted efficiently by the  $A^2\Pi_u \leftarrow X^2\Sigma_g^+$  transition whose transition dipole moment is perpendicular to the molecular axis, resulting in the significant increase in the air lasing signal. Furthermore, we revealed<sup>5</sup> that the extent of the population inversion can be increased further by combining the polarization-modulated 800 nm laser pulse with a 1.6  $\mu\text{m}$  IR pulse, which induces vibrational Raman transitions and depletes the population in the  $X^2\Sigma_g^+(v = 0)$  state to an almost empty level, leading to a giant enhancement of the lasing signal at 391 nm by 5 orders of magnitude.

## References

- 1) H. Xu, E. Lötstedt, A. Iwasaki, K. Yamanouchi, *Nat. Commun.* **6**, 8347 (2015).
- 2) T. Ando, E. Lötstedt, A. Iwasaki, H. Li, Y. Fu, S. Wang, H. Xu, K. Yamanouchi, *Phys. Rev. Lett.* **123**, 203201 (2019).
- 3) Y. Zhang, E. Lötstedt, T. Ando, A. Iwasaki, H. Xu, K. Yamanouchi, *Phys. Rev. A* **104**, 023107 (2021).
- 4) H. Li, M. Hou, H. Zang, Y. Fu, E. Lötstedt, T. Ando, A. Iwasaki, K. Yamanouchi, H. Xu, *Phys. Rev. Lett.* **122**, 013202 (2019).
- 5) H. Li, E. Lötstedt, H. Li, Y. Zhou, N. Dong, L. Deng, P. Lu, T. Ando, A. Iwasaki, Y. Fu, S. Wang, J. Wu, K. Yamanouchi, H. Xu, *Phys. Rev. Lett.* **125**, 053201 (2020).